Geochemistry, Geophysics, Geosystems

RESEARCH ARTICLE
10.1029/2020GC009129

Li Partitioning Into Coccoliths of *Emiliania huxleyi*: Evaluating the General Role of "Vital Effects" in Explaining Element Partitioning in Biogenic Carbonates

Gerald Langer[1], Aleksey Sadekov[2], Mervyn Greaves[3], Gernot Nehrke[4], Ian Probert[5], Sambuddha Misra[6], and Silke Thoms[4]

[1]The Marine Biological Association of the United Kingdom, The Laboratory, Citadel Hill, Plymouth, UK, [2]ARC Centre of Excellence for Coral Reef Studies, Ocean Graduate School, University of Western Australia, Crawley, Western Australia, Australia, [3]The Godwin Laboratory for Palaeoclimate Research, Department of Earth Sciences, University of Cambridge, Cambridge, UK, [4]Alfred Wegener Institute, Helmholtz Centre for Polar and Marine Research, Bremerhaven, Germany, [5]Sorbonne Université/Centre National de la Recherche Scientifique, Roscoff Culture Collection, FR2424, Station Biologique de Roscoff, Roscoff, France, [6]Centre for Earth Sciences, Indian Institute of Science, Bangalore, India

Key Points:
- The Li partitioning pattern of *E. huxleyi* resembles that of *A. lessonii* and inorganic calcite
- Li partitioning in *E. huxleyi* is dominated by a coupled transmembrane transport of Li and Ca
- The vital effect is ubiquitous in calcifying organisms, even if it appears to be absent

Correspondence to:
G. Langer,
gerlan@mba.ac.uk

Citation:
Langer, G., Sadekov, A., Greaves, M., Nehrke, G., Probert, I., Misra, S., & Thoms, S. (2020). Li partitioning into coccoliths of *Emiliania huxleyi*: Evaluating the general role of "vital effects" in explaining element partitioning in biogenic carbonates. *Geochemistry, Geophysics, Geosystems*, *21*, e2020GC009129. https://doi.org/10.1029/2020GC009129

Received 24 APR 2020
Accepted 11 JUN 2020
Accepted article online 14 JUN 2020

Abstract *Emiliania huxleyi* cells were grown in artificial seawater of different Li and Ca concentrations and coccolith Li/Ca ratios determined. Coccolith Li/Ca ratios were positively correlated to seawater Li/Ca ratios only if the seawater Li concentration was changed, not if the seawater Ca concentration was changed. This Li partitioning pattern of *E. huxleyi* was previously also observed in the benthic foraminifer *Amphistegina lessonii* and inorganically precipitated calcite. We argue that Li partitioning in both *E. huxleyi* and *A. lessonii* is dominated by a coupled transmembrane transport of Li and Ca from seawater to the site of calcification. We present a refined version of a recently proposed transmembrane transport model for Li and Ca. The model assumes that Li and Ca enter the cell via Ca channels, the Li flux being dependent on the Ca flux. While the original model features a linear function to describe the experimental data, our refined version uses a power function, changing the stoichiometry of Li and Ca. The version presented here accurately predicts the observed dependence of D_{Li} on seawater Li/Ca ratios. Our data demonstrate that minor element partitioning in calcifying organisms is partly mediated by biological processes even if the partitioning behavior of the calcifying organism is indistinguishable from that of inorganically precipitated calcium carbonate.

Plain Language Summary Marine shell-forming organisms such as the minute, but abundant, coccolithophores (single-celled phytoplankton) and foraminifera (single-celled zooplankton) are not only ecologically important but also contribute significantly to the global carbonate sink. Minor elements (e.g., Sr and Li) trapped in biogenic carbonate sediments provide a window into past environmental conditions such as temperature, which is relevant for climate change. An understanding of elemental incorporation processes is required in order to correctly translate these minor element signatures into past environmental data. Here we conducted culture experiments with the coccolithophore *Emiliania huxleyi* to determine its Li incorporation behavior. We compare our results with previously published data on the foraminifer *Amphistegina lessonii* and data on synthetic calcite. The Li incorporation behavior of biogenic calcites is surprisingly similar to that of synthetic calcite. This is usually taken to mean that Li incorporation into shells should proceed inorganically. By contrast, we conclude that minor element incorporation processes in marine shell-forming organisms always include biological processes. This is relevant to past climate reconstructions because it excludes any interpretation of minor element signatures in fossil shells based on inorganic processes only.

1. Introduction

Minor element (Me) incorporation into marine biogenic carbonates has been widely used to reconstruct environmental parameters such as temperature and seawater chemistry (Elderfield et al., 2000; Lea, 2014). For instance, seawater Sr/Ca ratios and Li/Ca ratios were reconstructed from foraminiferal Sr/Ca ratios and Li/Ca ratios, respectively (Delaney & Boyle, 1986; Hathorne & James, 2006; Lear et al., 2003). These

Table 1
Data Set Derived From the Experiments With E. huxleyi

Seawater										Coccoliths								
Li/Ca (mmol/mol)	Sr/Ca (mmol/mol)	(Ca) (mM)	(Li) (mM)	Li/Ca (μmol/mol) average	Li/Ca (μmol/mol) SD	Li/Ca (μmol/mol) SE	D_{Li} (L/mol) average	D_{Li} (L/mol) SD	D_{Li} (L/mol) SE	Sr/Ca (mmol/mol) average	Sr/Ca (mmol/mol) SD	Sr/Ca (mmol/mol) SE	DSr (mol/mol) average	DSr (mol/mol) SD	DSr (mol/mol) SE
Ca variable															
8.8778	1.8878	51.2997	0.4554	11.7804	2.3358	1.1679	0.0259	0.0051	0.0026	0.5470	0.0027	0.0013	0.2898	0.0014	0.0007
17.4384	3.6936	25.5100	0.4449	10.5786	1.9596	0.9798	0.0238	0.0044	0.0022	1.1411	0.0042	0.0021	0.3089	0.0011	0.0006
42.8061	8.9819	10.3055	0.4411	8.0220	0.2643	0.1321	0.0182	0.0006	0.0003	2.8930	0.0314	0.0157	0.3221	0.0035	0.0017
87.1270	18.1223	5.1587	0.4495	7.7428	0.3006	0.1503	0.0172	0.0007	0.0003	5.6569	0.0643	0.0321	0.3121	0.0035	0.0018
Li variable															
85.0525	8.6735	10.4984	0.8929	12.8377	0.9423	0.4712	0.0144	0.0011	0.0005	2.8073	0.0102	0.0059	0.3237	0.0012	0.0007
42.8061	8.9819	10.3055	0.4411	8.0220	0.2643	0.1321	0.0182	0.0006	0.0003	2.8930	0.0314	0.0157	0.3221	0.0035	0.0017
19.1934	8.6053	10.5258	0.2020	4.1315	0.2009	0.1005	0.0205	0.0010	0.0005	2.8021	0.0102	0.0051	0.3256	0.0012	0.0006
7.7179	8.6129	10.5816	0.0817	1.7705	0.0622	0.0311	0.0217	0.0008	0.0004	2.7468	0.0089	0.0063	0.3189	0.0010	0.0007

Note. SD = standard deviation, SE = standard error.

reconstructions assume a positive relationship between foraminiferal Me/Ca ratios and seawater Me/Ca ratios. Culture studies have shown that this assumption indeed holds true for Sr, not only in foraminifera but also in coccolithophores (Hermoso et al., 2017; Langer et al., 2006, 2016; Mejía et al., 2018; Müller et al., 2018). However, while Mg partitioning into foraminiferal calcite shows a behavior similar to that of Sr partitioning (Mewes et al., 2014, 2015), foraminiferal Li/Ca does not depend on seawater Li/Ca but on seawater Li concentration (Langer et al., 2015). At first glance this difference between divalent cation Sr (Mg) and the alkali metal ion Li could be explained in terms of inorganic precipitation processes. In contrast to divalent ions, alkali metal ions do not compete with Ca for a position in the calcite lattice (Busenberg & Plummer, 1985; Ishikawa & Ichikuni, 1984; Lorens, 1981; Marriott et al., 2004; Okumura & Kitano, 1986). However, any inorganic precipitation-based explanation of the minor element partitioning behavior of calcifying organisms has to face the persistent issue of the "vital effect," first mentioned by Urey et al. (1951): "We may ask whether there is a vital effect?"

The vital effect is usually discussed whenever there is a discrepancy between the minor element partitioning behavior of a calcifying organism and inorganic precipitation but often ignored when there is no discrepancy. In the latter case it is usually implied that minor element partitioning is driven by inorganic precipitation alone, but this might be mistaken. The U partitioning into foraminiferal calcite, for example, was first explained in terms of inorganic precipitation alone (Russell et al., 2004), but later inorganic precipitation combined with cellular U transport was suggested as an alternative explanation (Keul et al., 2013). This is where conceptual biomineralization models enter the debate. These models have been developed for different calcifiers based on a number of observations in various fields of research such as physiology, biochemistry, anatomy, ultrastructure, and elemental fractionation itself (Bentov et al., 2009; Erez, 2003; Erez & Braun, 2007; Gagnon et al., 2012; Langer et al., 2006; Mass et al., 2017; Nehrke et al., 2013; Simkiss & Wilbur, 1989; Tambutté et al., 2012; Vidavsky et al., 2016). The common feature of all these models is that they include biological processes in the overall partitioning mechanism of minor elements. They raise the question of the "invisible vital effect," in other words mimicry of inorganic partitioning behavior (Gussone et al., 2016; Keul et al., 2013; Taubner et al., 2012).

Li partitioning into foraminiferal calcite is a prime example. Although the pattern of Li partitioning into *Amphistegina lessonii* is explicable in terms of inorganic precipitation, an explanation based on transmembrane transport of ions was proposed (Langer et al., 2015). This explanation presupposes that foraminifera actually use transmembrane transport in order to deliver Ca ions to the site of calcification. However, even though several studies are in favor of this view (Glas et al., 2012; Keul et al., 2013; Langer et al., 2016; Mewes, Langer, Reichart, et al., 2015; Nehrke et al., 2013), there are still numerous studies proposing endocytosis of seawater as a mechanism by which Ca is transported to the site of calcification (Bentov et al., 2009; Erez, 2003; Evans et al., 2018). Coccolithophores, by contrast, solely use transmembrane transport to deliver Ca and other ions to the coccolith vesicle (Taylor & Brownlee, 2017). Here we ask the following question: Does the Li partitioning behavior of *Emiliania huxleyi* resemble that of *A. lessonii*? If the Li partitioning behavior of *E. huxleyi* was fundamentally different (dependence of coccolith Li/Ca on seawater Li/Ca) from that of *A. lessonii*, it would be highly likely that Li partitioning in this foraminifer is not driven by transmembrane transport. If the Li partitioning behavior of *E. huxleyi* was similar to that of *A. lessonii*, this would show that a transmembrane-based partitioning mechanism could produce the Li partitioning pattern we see in *A. lessonii*.

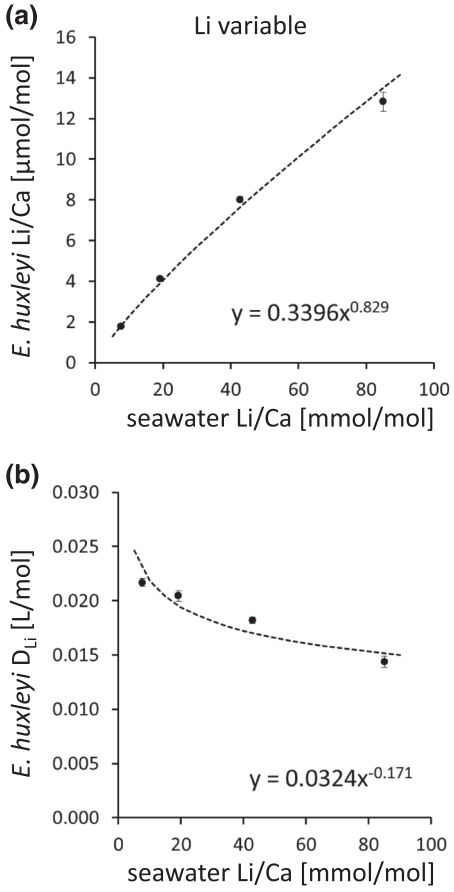

Figure 1. (a) *E. huxleyi* Li/Ca ratio (µmol/mol) versus seawater Li/Ca ratio (mmol/mol). The seawater Li/Ca ratio was changed by changing seawater Li concentration. The dashed line was calculated using the equation shown in the plot. Error bars represent standard error. (b) *E. huxleyi* D_{Li} (L/mol) versus seawater Li/Ca ratio (mmol/mol). The seawater Li/Ca ratio was changed by changing seawater Li concentration. The dashed line was calculated using the equation shown in the plot. Error bars represent standard error.

Since there are no published data on Li partitioning in coccolithophores, we conducted an experiment with *E. huxleyi*, similar in setup to the one performed on *A. lessonii* (Langer et al., 2015).

2. Material and Methods

2.1. Culture Experiments

Clonal cultures of *Emiliania huxleyi* (strain RCC3652) were obtained from the Roscoff Culture Collection (http://roscoff-culture-collection.org/) and grown in triplicate in sterile filtered (0.2 µm pore-size cellulose acetate filters) artificial seawater (for general composition of major ions except Ca see Langer et al., 2006, 2009; for particular changes to this composition with respect to Ca and Li see Table 1; all salts reagent grade, obtained from Merck) enriched with 100 µmol L^{-1} nitrate, 6.25 µmol L^{-1} phosphate, and trace metals and vitamins according to *f*/2 (Guillard & Ryther, 1962). The incident photon flux density was 250 µmol/m^2 s and a 16/8 hr light/dark cycle was applied. Experiments were carried out at 20°C. Two separate experiments were conducted. In one experiment the Li concentration of the artificial seawater was varied, and in the other experiment the Ca concentration of the artificial seawater was varied. For details on Li and Ca concentrations see Table 1. The pH of the artificial seawater was adjusted to 8.2 (NBS scale) by sodium hydroxide (0.1 M) addition. Seawater pH was determined potentiometrically using a glass electrode/reference electrode cell (Schott Instruments, Mainz, Germany), which included a temperature sensor and was two-point calibrated with National Bureau of Standards (NBS) buffers prior to every set of measurements. Average repeatability was ±0.02 pH units ($n = 30$). The salinity of the artificial seawater was determined by means of a conductivity meter (WTW Multi 340i) combined with a TetraCon 325 sensor. Cells were grown in dilute batch ensuring a quasi-constant carbonate chemistry over the course of the experiment (Langer et al., 2011). Cell densities were determined by means of flow cytometry. Cultures were harvested by filtering onto Omnipore polycarbonate membrane filters (0.8 µm pore-size) using a vacuum pump. The filters were dried at 50°C for 24 hr prior to storage at room temperature.

2.2. Sample Preparation and Determination of Me/Ca Ratios

Approximately 15–20 mg of the sample was subsampled from each filter by folding the filter with plastic tweezers and collecting flakes of material in 5 ml acid precleaned centrifuge tubes. To remove organic matter and residual seawater, 4 ml of 10% hydrogen peroxide was added to each sample tube and heated to ~60°C and ultrasonicated for 10 min. The sample was subsequently centrifuged to pellet the solid fraction and remove/exchange the residual solution. This procedure was repeated four times and followed by four rinses in water with ultrasonication and centrifugation in a similar way to the peroxide treatment. Type 1 (18.2 MOhm) purified water was used for all rinses. The rinses most likely only dissolved a negligible percentage of the sample, which does not affect the Li/Ca ratio (Yu et al., 2007).

We also left the samples in water for 12 hr as a final fifth rinse to further remove potential seawater contaminantion. Samples were left to dry after the final centrifugation and removal of the supernatant.

2.3. Analyses of Cultured *Emiliania huxleyi*

Subsamples of the prepared *Emiliania huxleyi* were transferred to 0.5 ml microcentrifuge tubes and rinsed a further time by adding 500 µl water, sonicating to mix the suspension and centrifuging. The supernatant water was removed and the samples dissolved in 500 µl 0.1 M HNO_3. The solution was centrifuged and 450 µl supernatant saved for analysis. A 25 µl aliquot was diluted tenfold for Ca determination by Inductively Coupled Plasma - Optical Emission Spectrophotometry (ICP-OES). The Ca concentrations confirmed that sample

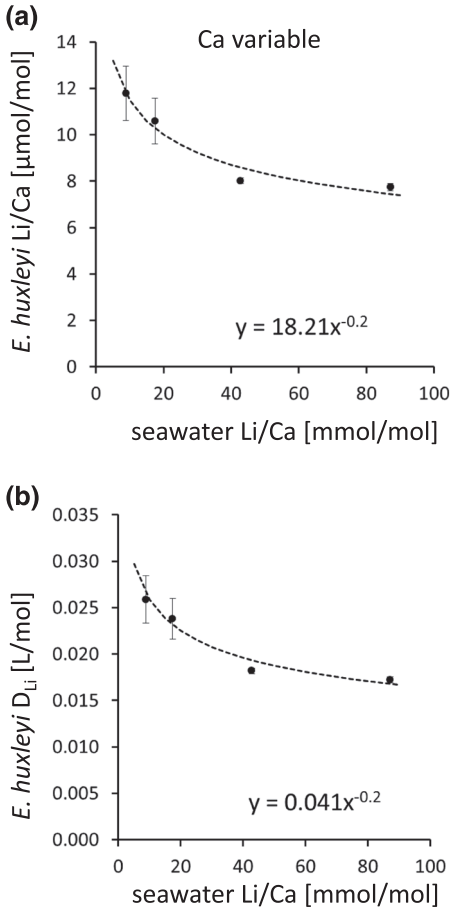

Figure 2. (a) *E. huxleyi* Li/Ca ratio (µmol/mol) versus seawater Li/Ca ratio (mmol/mol). The seawater Li/Ca ratio was changed by changing seawater Ca concentration. The dashed line was calculated using the equation shown in the plot. Error bars represent standard error. (b) *E. huxleyi* D_{Li} (L/mol) versus seawater Li/Ca ratio (mmol/mol). The seawater Li/Ca ratio was changed by changing seawater Ca concentration. The dashed line was calculated using the equation shown in the plot. Error bars represent standard error.

sizes ranging from 1.7 to 7.2 mg $CaCO_3$ had been dissolved. Aliquots of the remaining solution were diluted to constant Ca concentration for the determination of Li/Ca and Sr/Ca ratios. Sr/Ca was determined by ICP-OES using the method of de Villiers et al. (2002). Analytical precision for Sr/Ca is better than 0.3% relative standard deviation (r.s.d.), determined by replicate runs of a consistency standard containing 1.67 mmol/mol Sr/Ca.

Li/Ca ratios of *Emiliania huxleyi* were determined on a Thermo ElementXR sector field ICP-MS at the Department of Earth Sciences, University of Cambridge, following the method detailed in Misra et al. (2014). Long-term analytical precision for Li/Ca of 3.6% (1σ r.s.d.) has been established over a 4 year period, based on replicate measurements of an in-house foraminifera standard (CAM-Uvig-2) containing 13.5 µmol/mol Li/Ca.

2.4. Analyses of Culture Media

The culture media were analyzed in the same manner as previously for *A. lessonii* culture experiments (Langer et al., 2015). Briefly, Li/Ca and Sr/Ca ratios were determined by ICP-OES after dilution of the culture media to a constant sodium concentration of 110 ppm. Samples were run on a Varian Vista Axial ICP-OES using the 315.887 nm Ca, 421.552 nm Sr, and the 670.783 nm Li emission lines. Calibration standards were prepared from International Association for the Physical Sciences of the Ocean (IAPSO) standard seawater to closely match the concentration matrix of the media solutions, spiked with Ca, Li, and Sr (also Mg) to cover the concentration ranges in the experiments. Precision better than 0.5% (r.s.d.) was achieved for both Li/Ca and Sr/Ca, determined by replicate runs of a consistency standard containing 14.5 mmol/mol Li/Ca and 30.6 mmol/mol Sr/Ca.

3. Results and Discussion

Emiliania huxleyi was grown under different seawater Li as well as Ca concentrations. If the seawater Li/Ca is changed by altering Li concentration, coccolith Li/Ca is positively correlated to seawater Li/Ca (Figure 1). If, on the other hand, seawater Li/Ca is changed by adjusting the Ca concentration, coccolith Li/Ca is negatively correlated to seawater Li/Ca (Figure 2). This pattern is in stark contrast to the behavior of Sr, that is, changing the seawater Sr/Ca by changing seawater Ca concentration yields a positive correlation between coccolith Sr/Ca and seawater Sr/Ca (Figure 3). Our Sr data tally well with published data on both *E. huxleyi* and *Amphistegina lessonii* in the sense that calcite Sr/Ca depends on seawater Sr/Ca, as opposed to seawater Sr concentration (Langer et al., 2006, 2016). As a general caveat we point out that the number of data points used in our and similar studies (see above references and section 1) is not sufficient to run statistical significance tests. Nevertheless, the relationships described here and elsewhere are sufficiently unambiguous to justify the conclusions drawn. At any rate, it would be desirable to conduct additional studies in the future including more data points and statistical tests.

However, coccolith Li/Ca only increases if seawater Li concentration is increased, not if seawater Ca concentration is decreased. This pattern was also reported for *A. lessonii* (Langer et al., 2015). Hence, the Li partitioning pattern is the same in inorganically precipitated calcite (Marriott, Henderson, Belshaw, & Tudhope, 2004; Okumura & Kitano, 1986), *A. lessonii* (Langer et al., 2015) and *E. huxleyi* (this study). It is generally accepted that coccolithophores employ transmembrane transport to deliver Ca ions to the coccolith vesicle (Taylor & Brownlee, 2017), and interpretations of minor element and isotope partitioning into coccoliths have been based on conceptual biomineralization models featuring transmembrane transport of Ca and the minor element in question (Gussone et al., 2006; Langer et al., 2006, 2009; Stoll et al., 2012). We therefore propose that the similarity in partitioning pattern between inorganically precipitated calcite

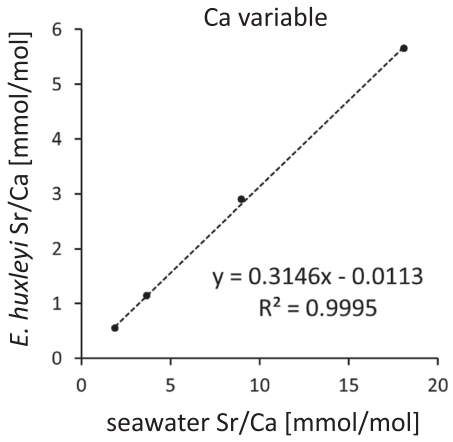

Figure 3. *E. huxleyi* Sr/Ca ratio (mmol/mol) versus seawater Sr/Ca ratio (mmol/mol). The seawater Sr/Ca ratio was changed by changing seawater Ca concentration. The dashed line is the linear trend line (equation and r^2 shown in the plot). The slope of the trend line represents the DSr = 0.3146. Error bars represent standard error.

and *E. huxleyi* coccoliths is not based on a similarity in partitioning mechanism but represents a case of mimicry; that is, transmembrane transport of Li and Ca in *E. huxleyi* creates a partitioning pattern that looks like that of inorganically precipitated calcite. Consequently, the Li partitioning pattern of *A. lessonii* could also represent a case of inorganic mimicry (Langer et al., 2015). To analyze the Li partitioning pattern in more detail, we adopt the model of a coupled transmembrane transport of Li and Ca proposed by Langer et al. (2015), which is based on the idea that Li can enter the cell via Ca channels. In Langer et al. (2015), the authors used a linear function to describe their experimental data. While this is possible also for *E. huxleyi*, a more in-depth qualitative analysis of the data, both *E. huxleyi* and *A. lessonii*, leads us to conclude that a power function serves the purpose better. The usage of a power function does not change the underlying idea of the model but merely the stoichiometry of the Li and Ca transport. According to the model, the Li flux (F_{Li}) is

$$F_{\mathrm{Li}} = k[\mathrm{Li}]^{x}_{\mathrm{SW}}[\mathrm{Ca}]^{y}_{\mathrm{SW}} \tag{1}$$

As suggested in Langer et al. (2015), the Ca flux is probably not significantly affected by the Li ion due to the small size of the latter and is therefore described as

$$F_{\mathrm{Ca}} = l[\mathrm{Ca}]_{\mathrm{SW}} \tag{2}$$

which is a valid description for the channels as well as for a nonsaturated active transport process. Then, the Li/Ca of the precipitated calcite is given by the ratio of the ion fluxes:

$$\left(\frac{\mathrm{Li}}{\mathrm{Ca}}\right)_{CC} = \frac{F_{\mathrm{Li}}}{F_{\mathrm{Ca}}} = \frac{k}{l}[\mathrm{Ca}]^{y-1}_{\mathrm{SW}}[\mathrm{Li}]^{x}_{\mathrm{SW}} = \frac{k}{l}[\mathrm{Ca}]^{y-1+x}R^{x}_{\mathrm{SW}} \tag{3}$$

where R_{SW} is the seawater Li/Ca. To illustrate the advantage of a power function, we replotted the *A. lessonii* data against R_{SW} and applied equation 3, as we did for *E. huxleyi* (Figure 1). Equation 3 indicates that the calcite Li/Ca is correlated to R_{SW} with a positive power (x = 0.829) only if the Li concentration of seawater is changed. From the last term in equation 3 follows the observed power function describing the positive correlation between the calcite Li/Ca and the seawater Li/Ca at constant Ca concentration:

$$\left(\frac{\mathrm{Li}}{\mathrm{Ca}}\right)_{CC} = \frac{k}{l}[\mathrm{Ca}]^{y-1+x}_{\mathrm{SW}}R^{x}_{\mathrm{SW}} = const_1 R^{x}_{\mathrm{SW}} \tag{4}$$

However, if the Ca concentration of seawater is changed, while keeping Li concentration constant, the calcite Li/Ca is negatively correlated to R_{SW}, which is indicated by a negative power ($1 - y = -0.2$) in equation 5:

$$\left(\frac{\mathrm{Li}}{\mathrm{Ca}}\right)_{CC} = \frac{k}{l}[\mathrm{Li}]^{x+y-1}_{\mathrm{SW}}R^{1-y}_{\mathrm{SW}} = const_2 R^{1-y}_{\mathrm{SW}} \tag{5}$$

The change in the Li partitioning coefficient D_{Li} with changing seawater Li/Ca for both experimental setups can immediately be derived by using Equations 4 and 5, respectively. If the Li concentration of seawater is changed, it follows from Equation 4 a power function for the relationship between D_{Li} and R_{SW}:

$$D_{\mathrm{Li}} = \frac{1}{[\mathrm{Li}]_{\mathrm{SW}}}\left(\frac{\mathrm{Li}}{\mathrm{Ca}}\right)_{CC} = \frac{const_1}{[\mathrm{Ca}]_{\mathrm{SW}}}R^{x-1}_{\mathrm{SW}} = const_3 R^{x-1}_{\mathrm{SW}} \tag{6}$$

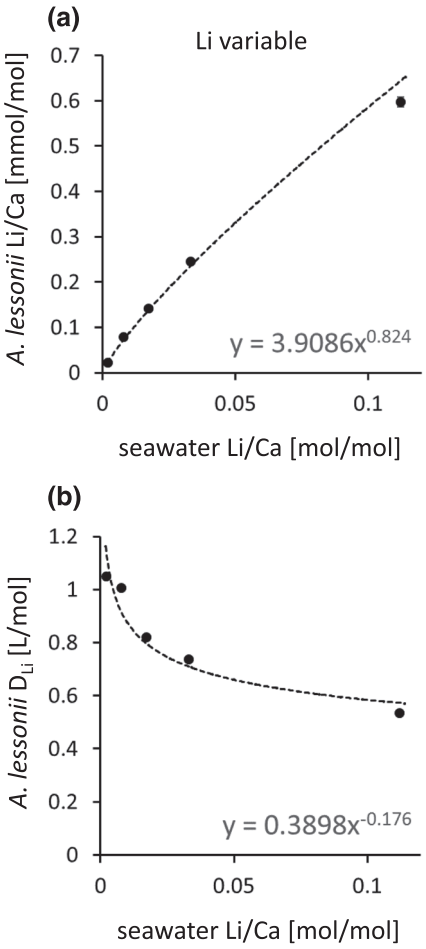

Figure 4. (a) *A. lessonii* Li/Ca ratio (mmol/mol) versus seawater Li/Ca ratio (mol/mol). The seawater Li/Ca ratio was changed by changing seawater Li concentration. The dashed line was calculated using the equation shown in the plot. Error bars represent standard error. Data from Langer et al. (2015). (b) *A. lessonii* D_{Li} (L/mol) versus seawater Li/Ca ratio (mol/mol). The seawater Li/Ca ratio was changed by changing seawater Li concentration. The dashed line was calculated using the equation shown in the plot. Error bars represent standard error. Data from Langer et al. (2015).

For the case of changing Ca concentration, the power function for D_{Li} is given by

$$D_{Li} = \frac{1}{[Li]_{SW}}\left(\frac{Li}{Ca}\right)_{CC} = \frac{const_2}{[Li]_{SW}} R_{SW}^{1-y} = const_4 R_{SW}^{1-y} \quad (7)$$

Here, two features are particularly interesting. First, the model curves describe not only the correlation between calcite Li/Ca and seawater Li/Ca, but the predicted change in D_{Li} with changing seawater Li/Ca fits the experimental data. Second, the relationships in *A. lessonii* and *E. huxleyi* are remarkably similar (Figures 1 and 4). This similarity points to a similar underlying mechanism. We emphasize that this similarity does not prove a common Li partitioning mechanism in *A. lessonii* and *E. huxleyi*, but it renders a common mechanism possible and even likely. We propose that this common mechanism is dominated by coupled transmembrane transport of Li and Ca, as suggested by Langer et al. (2015).

However, despite the striking similarity in Li partitioning patterns of *A. lessonii* and *E. huxleyi*, there are also differences. If the seawater Li/Ca is changed by altering seawater Ca concentration, the *A. lessonii* Li/Ca ratio remains constant, whereas the *E. huxleyi* Li/Ca ratio increases at low seawater Li/Ca (Langer et al., 2015, and Figure 2). The reason for this could be the bigger range in seawater Li/Ca in the *E. huxleyi* experiment. Regardless of the reason for this difference, the important observation here is that in both *A. lessonii* and *E. huxleyi* there is no positive correlation between calcite Li/Ca and seawater Li/Ca if the latter is changed by changing seawater Ca concentration, in contrast to divalent cations such as Sr and Mg (this study; Langer et al., 2006, 2016; Mewes et al., 2014, 2015; Mewes, Langer, Reichart, et al., 2015). This underlines that in both *A. lessonii* and *E. huxleyi* the alkali metal Li behaves differently from the divalent cations Sr and Mg.

The other difference between the Li partitioning behavior of *A. lessonii* and *E. huxleyi* concerns the partitioning coefficient D_{Li}. The partitioning coefficient of a minor element (Me) is usually calculated according to $D_{Me} = (Me/Ca)_{cc}/(Me/Ca)_{sw}$ (e.g., Lorens, 1981). While this definition works well for divalent cations, the D_{Me} of alkali cations such as Li should be calculated according to $D_{Me} = (Me/Ca)_{cc}/[Me]_{sw}$ (Busenberg & Plummer, 1985; Langer et al., 2015; Okumura & Kitano, 1986). However, even some recent studies still use the former definition of the partitioning coefficient for alkali metal ions (Evans et al., 2018; Füger et al., 2019). In order to put our *E. huxleyi* D_{Li} in the context of literature data, we therefore use both definitions of D_{Li}. From Figure 5 the following conclusions may be drawn: (1) *A. lessonii* D_{Li} is higher than *E. huxleyi* D_{Li}, (2) different foraminifera have similar D_{Li}, (3) *E. huxleyi* D_{Li} falls within the range of values for inorganic calcite, and (4) *A. lessonii* D_{Li} is higher than the one of inorganic calcite.

Please note that values for $D_{Li} = (Li/Ca)_{cc}/(Li/Ca)_{sw}$ are potentially misleading, even when only used as relative values. This is due to the variable Ca concentration used in different experiments. However, only Conclusion 2 (see above) relies on this potentially misleading definition of D_{Li} alone. We are therefore cautious with respect to Conclusion 2 but confident with respect to Conclusions 1, 3, and 4. Taken together with the other data discussed above, this comparison of different D_{Li} suggests that *E. huxleyi* displays a complete mimicry of inorganic Li partitioning behavior, whereas *A. lessonii* does so only partially; that is, the *A. lessonii* D_{Li} differs from the inorganic one. The question of whether the latter difference is indicative of a fundamental difference in partitioning mechanism between *A. lessonii* and *E. huxleyi*, or is merely indicative of different membrane characteristics (e.g., calcium channels, White, 2000), cannot be answered with certainty. However, the absolute Li fractionation of, for example, Ca channels in the plasma membrane

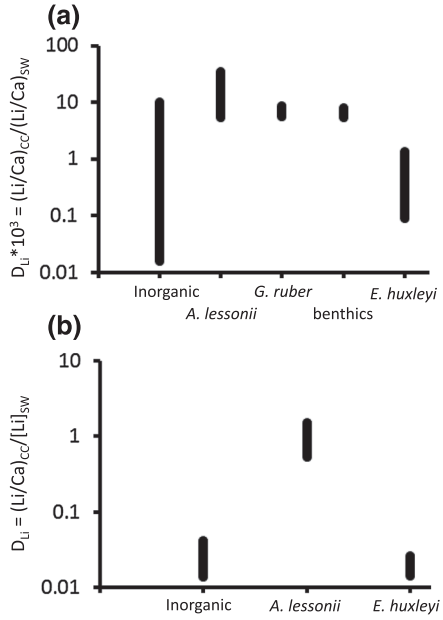

Figure 5. (a) $D_{Li}*10^3$ = (Li/Ca)cc/$(Li/Ca)_{sw}$ of different calcites. Data were taken from the following: inorganic: Okumura and Kitano (1986), Marriott, Henderson, Belshaw, and Tudhope (2004), Marriott et al. (2004), and Füger et al. (2019). *A. lessonii*: Langer et al. (2015). *Globigerinoides ruber*: Evans et al. (2018). Benthics: Marriott, Henderson, Belshaw, and Tudhope (2004). *E. huxleyi*: this study. (b) D_{Li} = (Li/Ca)cc/$[Li]_{sw}$ of different calcites. Data were taken from the following: inorganic: Okumura and Kitano (1986) and Marriott, Henderson, Crompton, et al. (2004). *A. lessonii*: Langer et al. (2015). *E. huxleyi*: this study.

of foraminifera might well be different from that of coccolithophores. This difference would be sufficient to explain the difference in D_{Li} between *A. lessonii* and *E. huxleyi*, without the need to invoke a fundamental difference in fractionation mechanism such as different cellular pathways for Li and Ca, for example, vesicle transport in foraminifera and transmembrane transport in coccolithophores. Taken together with other support for Ca and minor element transmembrane transport in foraminifera (Glas et al., 2012; Keul et al., 2013; Langer et al., 2016; Mewes, Langer, Reichart, et al., 2015; Nehrke et al., 2013), we conclude that there is no fundamental difference in Li partitioning mechanism between *A. lessonii* and *E. huxleyi*. The most plausible interpretation is that both species feature a coupled transmembrane transport of Li and Ca, accounting for the Li partitioning behavior described above. However, transmembrane transport of Li and Ca in *A. lessonii* does not exclude additional fractionation steps such as a precursor phase (Jacob et al., 2017), which would introduce a constant offset of the curves but not change their shapes. The need to combine physiological and mineralogical fractionation steps in a description of the minor element incorporation behavior of *A. lessonii* was previously highlighted for the divalent cation Mg (Langer et al., 2016; Mewes, Langer, Thoms, et al., 2015). The discovery of a metastable precursor phase for shell calcite in foraminifera (Jacob et al., 2017) could perhaps explain why D_{Li} in *A. lessonii* is different from that of *E. huxleyi*, because there is currently no evidence for a precursor phase in coccolithophores.

4. Conclusion

This study indicates that the issue of the vital effect is omnipresent in calcifying organisms, even when the partitioning behavior of the organism in question is indistinguishable from that of inorganically precipitated calcium carbonate. We do not conclude that every calcifying organism actually does show a vital effect, but we conclude that a vital effect cannot be excluded in any organism based on minor element partitioning data. The latter conclusion is based on the observation that *E. huxleyi* shows a complete mimicry of inorganic partitioning behavior, although its calcification mechanism is substantially different from inorganic precipitation. While these conclusions can be confidently drawn from our data, the number of data points puts limits on statistical significance tests which would make the exact relationships more robust. Future studies should therefore include more data points so that statistical significance tests can be performed.

Data Availability Statement

All data supporting the conclusions can be obtained from the MBA data repository (DOI https://doi.org/10.17031/ykdq-wy51).

Acknowledgments
This work was supported by the Natural Environment Research Council (NE/N011708/1).

References

Bentov, S., Brownlee, C., & Erez, J. (2009). The role of seawater endocytosis in the biomineralization process in calcareous foraminifera. *Proceedings of the National Academy of Sciences of the United States of America*, *106*(51), 21500–21504. https://doi.org/10.1073/pnas.0906636106

Busenberg, E., & Plummer, L. N. (1985). Kinetic and thermodynamic factors controlling the distribution of SO_3^{2-} and Na^+ in calcites and selected aragonites. *Geochimica et Cosmochimica Acta*, *49*(3), 713–725. https://doi.org/10.1016/0016-7037(85)90166-8

de Villiers, S., Greaves, M., & Elderfield, H. (2002). An intensity ratio calibration method for the accurate determination of Mg/Ca and Sr/Ca of marine carbonates by ICP-AES. *Geochemistry, Geophysics, Geosystems*, *3*(1), 1001. https://doi.org/10.1029/2001GC000169

Delaney, M. L., & Boyle, E. A. (1986). Lithium in foraminiferal shells: Implications for high-temperature hydrothermal circulation fluxes and oceanic crustal generation rates. *Earth and Planetary Science Letters*, *80*, 91–105.

Elderfield, H., Cooper, M., & Ganssen, G. (2000). Sr/Ca in multiple species of planktonic foraminifera: Implications for reconstructions of seawater Sr/Ca. *Geochemistry, Geophysics, Geosystems*, *1*(11), 1017. https://doi.org/10.1029/1999GC000031

Erez, J. (2003). The source of ions for biomineralization in foraminifera and their implications for paleoceanographic proxies. *Reviews in Mineralogy and Geochemistry*, *54*(1), 115–149. https://doi.org/10.2113/0540115

Erez, J., & Braun, A. (2007). Calcification in hermatypic corals is based on direct seawater supply to the biomineralization site. *Geochimica et Cosmochimica Acta*, *71*(15 Suppl 1), A260.

Evans, D., Müller, W., & Erez, J. (2018). Assessing foraminifera biomineralisation models through trace element data of cultures under variable seawater chemistry. *Geochimica et Cosmochimica Acta*, *236*, 198–217. https://doi.org/10.1016/j.gca.2018.02.048

Füger, A., Konrad, F., Leis, A., Dietzel, M., & Mavromatis, V. (2019). Effect of growth rate and pH on lithium incorporation in calcite. *Geochimica et Cosmochimica Acta*, *248*, 14–24. https://doi.org/10.1016/j.gca.2018.12.040

Gagnon, A. C., Adkins, J. F., & Erez, J. (2012). Seawater transport during coral biomineralization. *Earth and Planetary Science Letters*, *329–330*, 150–161.

Glas, M. S., Langer, G., & Keul, N. (2012). Calcification acidifies the microenvironment of a benthic foraminifer (*Ammonia* sp.). *Journal of Experimental Marine Biology and Ecology*, *424-425*, 53–58. https://doi.org/10.1016/j.jembe.2012.05.006

Guillard, R. R. L., & Ryther, J. H. (1962). Studies of marine planktonic diatoms, I, *Cyclotella nanna* (Hustedt) and *Detonula convervacea* (Cleve). *Canadian Journal of Microbiology*, *8*(2), 229–239. https://doi.org/10.1139/m62-029

Gussone, N., Filipsson, H., & Kuhnert, H. (2016). Mg/Ca, Sr/Ca and Ca isotope ratios in benthonic foraminifers related to test structure, mineralogy and environmental controls. *Geochimica et Cosmochimica Acta*, *173*, 142–159. https://doi.org/10.1016/j.gca.2015.10.018

Gussone, N., Langer, G., Thoms, S., Nehrke, G., Eisenhauer, A., Riebesell, U., & Wefer, G. (2006). Cellular calcium pathways and isotope fractionation in *Emiliania huxleyi*. *Geology*, *34*(8), 625–628. https://doi.org/10.1130/G22733.1

Hathorne, E. C., & James, R. H. (2006). Temporal record of lithium in seawater: A tracer for silicate weathering? *Earth and Planetary Science Letters*, *246*, 393–406.

Hermoso, M., Lefeuvre, B., Minoletti, F., & de Rafélis, M. (2017). Extreme strontium concentrations reveal specific biomineralization pathways in certain coccolithophores with implications for the Sr/Ca paleoproductivity proxy. *PLoS ONE*, *12*(10), e0185655. https://doi.org/10.1371/journal.pone.0185655

Ishikawa, M., & Ichikuni, M. (1984). Uptake of sodium and potassium by calcite. *Chemical Geology*, *42*(1-4), 137–146. https://doi.org/10.1016/0009-2541(84)90010-X

Jacob, D. E., Wirth, R., Agbaje, O. B. A., Branson, O., & Eggins, S. M. (2017). Planktic foraminifera form their shells via metastable carbonate phases. *Nature Communications*, *8*(1), 1265. https://doi.org/10.1038/s41467-017-00955-0

Keul, N., Langer, G., de Nooijer, L. J., Nehrke, G., Reichart, G.-J., & Bijma, J. (2013). Incorporation of uranium in benthic foraminiferal calcite reflects seawater carbonate ion concentration. *Geochemistry, Geophysics, Geosystems*, *14*, 102–111. https://doi.org/10.1029/2012GC004330

Langer, G., Gussone, N., Nehrke, G., Riebesell, U., Eisenhauer, A., Kuhnert, H., et al. (2006). Coccolith strontium to calcium ratios in *Emiliania huxleyi*: The dependence on seawater strontium and calcium concentrations. *Limnology and Oceanography*, *51*(1), 310–320. https://doi.org/10.4319/lo.2006.51.1.0310

Langer, G., Nehrke, G., Thoms, S., & Stoll, H. (2009). Barium partitioning in coccoliths of *Emiliania huxleyi*. *Geochimica et Cocmochimica Acta*, *73*(10), 2899–2906. https://doi.org/10.1016/j.gca.2009.02.025

Langer, G., Probert, I., Nehrke, G., & Ziveri, P. (2011). The morphological response of *Emiliania huxleyi* to seawater carbonate chemistry changes: An inter-strain comparison. *Journal of Nannoplankton Research*, *32*, 27–32.

Langer, G., Sadekov, A., Thoms, S., Keul, N., Nehrke, G., Mewes, A., et al. (2016). Sr partitioning in the benthic foraminifera *Ammonia aomoriensis* and *Amphistegina lessonii*. *Chemical Geology*, *440*, 306–312. https://doi.org/10.1016/j.chemgeo.2016.07.018

Langer, G., Sadekov, A., Thoms, S., Mewes, A., Nehrke, G., Greaves, M., et al. (2015). Li partitioning in the benthic foraminifera *Amphistegina lessonii*. *Geochemistry, Geophysics, Geosystems*, *16*, 4275–4279. https://doi.org/10.1002/2015GC006134

Lea, D. W. (2014). Elemental and isotopic proxies of past ocean temperatures. In H. D. Holland, & K. K. Turekian (Eds.), *Treatise on geochemistry* (Second ed., Vol. 8, pp. 373–397). Oxford: Elsevier. https://doi.org/10.1016/B978-0-08-095975-7.00614-8

Lear, C. H., Elderfield, H., & Wilson, P. A. (2003). A Cenozoic seawater Sr/Ca record from benthic foraminiferal calcite and its application in determining global weathering fluxes. *Earth and Planetary Science Letters*, *208*, 69–84.

Lorens, R. B. (1981). Sr, Cd, Mn and Co distribution coefficients in calcite as a function of calcite precipitation rate. *Geochimica et Cosmochimica Acta*, *45*(4), 553–561. https://doi.org/10.1016/0016-7037(81)90188-5

Marriott, C. S., Henderson, G. M., Belshaw, N. S., & Tudhope, A. W. (2004). Temperature dependence of δ^7Li, δ^{44}Ca and Li/Ca during growth of calcium carbonate. *Earth and Planetary Science Letters*, *222*(2), 615–624. https://doi.org/10.1016/j.epsl.2004.02.031

Marriott, C. S., Henderson, G. M., Crompton, R., Staubwasser, M., & Shaw, S. (2004). Effect of mineralogy, salinity, and temperature on Li/Ca and Li isotope composition of calcium carbonate. *Chemical Geology*, *212*(1-2), 5–15. https://doi.org/10.1016/j.chemgeo.2004.08.002

Mass, T., Giuffre, A. J., Sun, C.-Y., Stifler, C. A., Frazier, M. J., Neder, M., et al. (2017). Proceedings of the. *National Academy of Sciences of the United States of America*, *114*(37), E7670–E7678. https://doi.org/10.1073/pnas.1707890114

Mejía, L. M., Paytan, A., Eisenhauer, A., Böhm, F., Kolevica, A., Bolton, C., et al. (2018). Controls over $\delta^{44}/^{40}$Ca and Sr/Ca variations in coccoliths: New perspectives from laboratory cultures and cellular models. *Earth and Planetary Science Letters*, *481*, 48–60. https://doi.org/10.1016/j.epsl.2017.10.013

Mewes, A., Langer, G., de Nooijer, L. J., Bijma, J., & Reichart, G.-J. (2014). Effect of different seawater Mg^{2+} concentrations on calcification in two benthic foraminifers. *Marine Micropaleontology*, *113*, 56–64. https://doi.org/10.1016/j.marmicro.2014.09.003

Mewes, A., Langer, G., Reichart, G.-J., de Nooijer, L. J., Nehrke, G., & Bijma, J. (2015). The impact of Mg contents on Sr partitioning in benthic foraminifers. *Chemical Geology*, *412*, 92–98. https://doi.org/10.1016/j.chemgeo.2015.06.026

Mewes, A., Langer, G., Thoms, S., Nehrke, G., Reichart, G.-J., de Nooijer, L. J., & Bijma, J. (2015). Impact of seawater Ca^{2+} on the calcification and calcite Mg/Ca of *Amphistegina lessonii*. *Biogeosciences*, *12*(7), 2153–2162. https://doi.org/10.5194/bg-12-2153-2015

Misra, S., Greaves, M., Owen, R., Kerr, J., Elmore, A. C., & Elderfield, H. (2014). Determination of B/Ca of natural carbonates by HR-ICP-MS. *Geochemistry, Geophysics, Geosystems*, *15*, 1617–1628. https://doi.org/10.1002/2013GC005049

Müller, M. N., Krabbenhöft, A., Vollstaedt, H., Brandini, F. P., & Eisenhauer, A. (2018). Stable isotope fractionation of strontium in coccolithophore calcite: Influence of temperature and carbonate chemistry. *Geobiology*, *16*(3), 297–306. https://doi.org/10.1111/gbi.12276

Nehrke, G., Keul, N., Langer, G., de Nooijer, L. J., Bijma, J., & Meibom, A. (2013). A new model for biomineralization and trace-element signatures of foraminifera tests. *Biogeosciences*, *10*(10), 6759–6767. https://doi.org/10.5194/bg-10-6759-2013

Okumura, M., & Kitano, Y. (1986). Coprecipitation of alkali metal ions with calcium carbonate. *Geochimica et Cosmochimica Acta*, *50*(1), 49–58. https://doi.org/10.1016/0016-7037(86)90047-5

Russell, A. D., Hönisch, B., Spero, H. J., & Lea, D. W. (2004). Effects of seawater carbonate ion concentration and temperature on shell U, Mg, and Sr in cultured planktonic foraminifera. *Geochimica et Cosmochimica Acta*, *68*(21), 4347–4361. https://doi.org/10.1016/j.gca.2004.03.013

Simkiss, K., Wilbur, K., & Biomineralization (1989). *Cell biology and mineral deposition*. San Diego: Academic Press.
Stoll, H., Langer, G., Shimizu, N., & Kanamaru, K. (2012). B/Ca in coccoliths and relationship to calcification vesicle pH and dissolved inorganic carbon concentrations. *Geochimica et Cosmochimica Acta*, *80*, 143–157. https://doi.org/10.1016/j.gca.2011.12.003
Tambutté, E., Tambutté, S., Segonds, N., Zoccola, D., Venn, A., Erez, J., & Allemand, D. (2012). Calcein labelling and electrophysiology: Insights on coral tissue permeability and calcification. *Proceedings of the Biological Sciences*, *279*(1726), 19–27. https://doi.org/10.1098/rspb.2011.0733
Taubner, I., Böhm, F., Eisenhauer, A., Garbe-Schönberg, D., & Erez, J. (2012). Uptake of alkaline earth metals in Alcyonarian spicules (Octocorallia). *Geochimica et Cosmochimica Acta*, *84*, 239–255. https://doi.org/10.1016/j.gca.2012.01.037
Taylor, A. R., & Brownlee, C. (2017). Glen wheeler (2017) Coccolithophore cell biology: Chalking up progress. *Annual Review of Marine Science*, *9*(1), 283–310. https://doi.org/10.1146/annurev-marine-122414-034032
Urey, H. C., Lowenstam, H. A., Epstein, S., & McKinney, C. R. (1951). Measurement of paleo-temperatures and temperatures of the uppercretaceous of England, Denmark, and the southeastern United-States. *Geological Society of America Bulletin*, *62*, 399–416.
Vidavsky, N., Addadi, S., Schertel, A., Ben-Ezra, D., Shpigel, M., Addadi, L., & Weiner, S. (2016). Calcium transport into the cells of the sea urchin larva in relation to spicule formation. *Proceedings of the National Academy of Sciences of the United States of America*, *113*(45), 12637–12642. https://doi.org/10.1073/pnas.1612017113
White, P. J. (2000). Calcium channels in higher plants. *Biochimica et Biophysica Acta (BBA)-biomembranes*, *1465*, 171–189.
Yu, J., Elderfield, H., Greaves, M., & Day, J. (2007). Preferential dissolution of benthic foraminiferal calcite during laboratory reductive cleaning. *Geochemistry, Geophysics, Geosystems*, *8*, Q06016. https://doi.org/10.1029/2006GC001571